# NATIONAL ADVISORY COMMITTEE FOR AERONAUTICS

## TECHNICAL NOTE 4222

DROP-SIZE DISTRIBUTIONS FOR IMPINGING-JET BREAKUP

IN AIRSTREAMS SIMULATING THE VELOCITY

CONDITIONS IN ROCKET COMBUSTORS

By Robert D. Ingebo

Lewis Flight Propulsion Laboratory
Cleveland, Ohio

NACA

Washington

March 1958

MAR 18 1958

NATIONAL ADVISORY COMMITTEE FOR AERONAUTICS

TECHNICAL NOTE 4222

DROP-SIZE DISTRIBUTIONS FOR IMPINGING-JET BREAKUP IN AIRSTREAMS

SIMULATING THE VELOCITY CONDITIONS IN ROCKET COMBUSTOR.

By Robert D. Ingebo

## SUMMARY

Drop-size-distribution data were obtained for heptane sprays produced by pairs of impinging jets in airstreams over ranges of orifice diameter $D_j$, liquid-jet velocity $V_j$, and velocity difference between the airstream and the liquid jet $\Delta V$. All drop-size-distribution data were analyzed by using the Nukiyama-Tanasawa expression

$$\frac{dR}{dD} = \left(\frac{3.915}{D_{30}}\right)^6 \frac{D^5}{120} e^{-3.915 \, D/D_{30}}$$

where $R$ is the volume fraction of drops having diameters $<D$, and $D_{30}$ is the volume-number-mean drop diameter. By using values of $D_{30}$ obtained from this expression, the following empirical expression was obtained:

$$D_j/D_{30} = 2.64 \sqrt{D_j V_j} + 0.97 \, D_j \Delta V$$

where diameters and velocities are expressed in inches and feet per second, respectively.

## INTRODUCTION

The specific impulse obtained for a given fuel and oxidant combination is a function of the completeness of burning in the rocket combustor. In the case of a hydrocarbon - liquid oxygen propellant combination, the relatively low vaporization rate of the hydrocarbon may limit the completeness of burning and hence the performance of the engine. In reference 1, vaporization-rate equations based on assumed drop-size distributions for hydrocarbon sprays are integrated with the aid of digital computers, and rocket engine performance is related to atomization and vaporization. However, quantitative performance values could not be predicted from the

results, primarily because of lack of knowledge of the drop-size distributions produced by rocket injectors. If drop-size distributions were known, vaporization-rate equations could be applied more rigorously to predicting rocket engine performance. Accordingly, the purpose of this study was to obtain drop-size-distribution data for a rocket injector similar to that used in reference 1. A nonburning airstream environment of relatively low temperature and pressure was used to simulate rocket-combustor velocity conditions.

Several investigators have photographed sprays produced by pairs of impinging jets (ref. 2) to obtain spray-pattern photographs. However, their methods did not yield drop-size-distribution data. Dr. Tanasawa (ref. 3) has studied "flat impingement" (180° impingement of opposing jets) in "still air" and has obtained drop-size-distribution data. In the present study pairs of 90° impinging jets were used.

Drop-size-distribution data previously have been obtained for cross-current breakup of liquid jets in airstreams by means of a high-speed camera (refs. 4 and 5). The same camera equipment was used in the present investigation to study the breakup of impinging n-heptane jets in airstreams simulating rocket-combustor velocity conditions. Accordingly, drop-size-distribution data were obtained for ranges of injector-orifice diameter, liquid-jet velocity, and velocity difference between the airstream and the liquid jets. Finally, an empirical drop-size-distribution expression was derived from an analysis of the data.

<div align="center">SYMBOLS</div>

a    mean diameter notation

b    constant (eq. (3)), $cm^{-1}$

c    mean diameter notation

D    drop diameter, cm

$D_j$    injector-orifice diameter, cm

$\bar{D}$    constant (eq. (2)), cm

$D^*$    constant (eq. (1)), cm

$D_{30}$    volume-number-mean drop diameter defined by the general expression

$$D_{ac}^{a-c} = \frac{\Sigma n D^a}{\Sigma n D^c}, \quad \text{where} \quad D_{30} = (\Sigma n D^3/\Sigma n)^{1/3}$$

4759

$K_1$     proportionality constant, $(\text{sec}/\text{cm}^2)^{1/2}$

$K_2$     proportionality constant, $\text{sec}/\text{cm}^2$

$n$     number of drops in given size range, $\Delta D$

$q$     constant

$R$     volume fraction of drops having diameters $< D$

$V_j$     injection velocity (same for each jet in given pair), cm/sec

$\Delta V$     velocity difference between airstream and liquid jets (always positive), cm/sec

$y$     $\ln (D/D^{*})$

$\delta$     constant

Subscript:

$0$     condition where $\Delta V = 0$

## APPARATUS AND PROCEDURE

A diagram of the test section and equipment used to study the breakup of pairs of impinging n-heptane jets in airstreams is shown in figure 1. The airstream temperature and static pressure were $82^{\circ} \pm 3^{\circ}$ F and 29.3 inches of mercury, respectively. A sketch of the $90^{\circ}$ impinging-jet injectors, which were similar to that used in reference 1, is shown in figure 2. n-Heptane was injected into the 4- by 12-inch test section with the impinging-jet injector directed downstream so that the flat sheet of liquid formed on impact was in a plane parallel to the pyrex glass windows. Each window was attached to a 3-inch-diameter steel pipe "stub", 3 inches in length, containing 1/4-inch copper-tubing coils. Steam was passed through the coils to vaporize liquid entering the "stubs" and thus keep the windows clear while photographing the spray.

The high-speed camera shown in figure 1 and described in reference 5 was positioned at several distances downstream from the injector. Figure 3 shows an illustration and typical photomicrographs of the breakup of n-heptane jets taken at distances of 1, 3, 5, and 8 inches downstream from the point of impingement. In a distance of 1 inch, sheets were formed with waves whose crests began to break up and form ligaments within 3 inches. At a distance of 5 inches, ligaments were still breaking up and drops were forming. Finally, at 8 inches the process of drop formation appeared complete.

Drop-size-distribution data were obtained for each test condition
by measuring drop images on the photomicrographs with an accuracy of ±3
microns. Approximately 1400 drop images were measured for each test
condition; this gave a statistical error-factor of approximately $3\frac{1}{2}$ percent.

Photomicrographs were obtained for each test condition by traversing the
spray cross section with the objective plane of the camera positioned at
each of the 40 points shown in figure 1 (normal to the airflow and 8 in.
downstream from the point of impingement). The vertical positions were
obtained by raising and lowering the injector in increments of 1/2 inch,
and the horizontal positions were obtained by moving the camera toward
or away from the windows in increments of 1/2 inch.

## RESULTS AND DISCUSSION

Drop-size-distribution data were obtained for ranges of orifice
diameter, liquid-jet velocity, and velocity difference between the airstream
and the liquid jet. Also, maximum drop diameters were observed from
photomicrographs for each test and recorded in table I. These data
show that impinging-jet injectors produced relatively coarse sprays,
as shown in the following table:

| Type of atomization (with comparable size jets) | Maximum-observed drop diameter, microns | Volume-number-mean drop diameter, microns |
|---|---|---|
| 90° Impinging jets (table I, run 1) | 1160 | 347 |
| Crosscurrent breakup of jets (ref. 4, run 4) | 225 | 81 |

Run 8 in table I shows that, even with the smallest orifice diameter
(0.029-in.) and the highest velocity difference (235 ft/sec) used in
this study, the maximum-observed drop diameter for impinging-jet injectors
was 180 microns, and the volume-number-mean drop diameter was 68 microns.

In analyzing the drop-size-distribution data, the following expressions
for size distribution (ref. 6) were used:

Log probability,

$$R = \frac{\delta}{\sqrt{\pi}} \int_{-\infty}^{\delta y} e^{-\delta^2 y^2} \, dy \qquad (1)$$

Rosin-Rammler,

$$1 - R = e^{-(D/\bar{D})^q} \tag{2}$$

Nukiyama-Tanasawa,

$$\frac{dR}{dD} = \frac{b^6}{120} D^5 e^{-bD} \tag{3}$$

Figure 4 shows plots of experimental data using the three distribution expressions. Figure 4(a) gives a plot of experimental data using equation (1). As found in reference 4, curves are obtained instead of straight lines, and $\delta$ is not a constant. This limits the application of the log-probability expression, since $\delta$ must be a constant in order to integrate equation (1). Also, as found in reference 4, figure 4(b) shows that Rosin-Rammler plots of the data yield straight lines having slopes of approximately 3. This slope gives a volume-number-mean drop diameter $D_{30}$ equal to zero, a result that seriously limits the usefulness of the Rosin-Rammler expression.

Best results were obtained with the Nukiyama-Tanasawa expression (eq. (3)), which may be rewritten as follows:

$$\log \frac{\Delta R}{(\Delta D) D^5} = -1.7 \ D/D_{30} + \log \left[ (3.915/D_{30})^6/120 \right] \tag{4}$$

since integration of equation (3) gives $D_{30} = 3.915/b = -1.7/\text{slope}$. Thus, values for $D_{30}$ were determined from data plots of equation (4), as shown in figures 4(c), (d), and (e). All values of $D_{30}$ are recorded in table I.

For the first four runs given in table I, the velocity of the airstream and the liquid-jet velocity were set approximately equal, that is, $\Delta V = 0$. For constant airstream and liquid temperature and constant airstream static pressure, the relation between the mean diameter $D_{30}$, the orifice diameter $D_j$, and the jet velocity $V_j$ may be expressed as

$$(D_{30})_0 = \varphi(D_j, V_j) \tag{5}$$

where the subscript 0 stipulates the condition $\Delta V = 0$. A log-log plot of $(D_j/D_{30})_0$ against $D_j V_j$, as shown in figure 5, gives the relation

$$\left(\frac{D_j}{D_{30}}\right)_0 = K_1 (D_j V_j)^{1/2} \tag{6}$$

where $K_1$ is a proportionality constant having the units $(sec/cm^2)^{1/2}$.
The constant $K_1$ may be determined from figure 6, and equation (6) becomes

$$\left(\frac{D_j}{D_{30}}\right)_0 = 0.30(D_jV_j)^{1/2} \tag{7}$$

For the remaining set of runs given in table I, the velocity difference $\Delta V$ was varied. In this case, it was assumed that

$$\frac{D_j}{D_{30}} - \left(\frac{D_j}{D_{30}}\right)_0 = \Phi(D_j,\Delta V) \tag{8}$$

since $(D_j/D_{30})_0 = D_j/D_{30}$ when $\Delta V = 0$. A log-log plot of the relation given in equation (8) is shown in figure 7. Since the slope of this plot is unity, the following expression is obtained:

$$\frac{D_j}{D_{30}} - \left(\frac{D_j}{D_{30}}\right)_0 = K_2 D_j \Delta V \tag{9}$$

where $K_2$ is a proportionality constant having the units $sec/cm^2$.
From the plot in figure 8, equation (9) becomes

$$\frac{D_j}{D_{30}} = 0.30(D_jV_j)^{1/2} + 0.0125\ D_j\Delta V \tag{10a}$$

when expressed in metric units of measure. In English units the equation is

$$\frac{D_j}{D_{30}} = 2.64(D_jV_j)^{1/2} + 0.97\ D_j\Delta V \tag{10b}$$

where $D_j$ and $D_{30}$ are expressed in inches, and $V_j$ and $\Delta V$ are expressed in feet per second. This expression shows little effect of orifice diameter when the velocity difference $\Delta V$ is very high. For the case of atomization of impinging jets in "still air", that is, $\Delta V = V_j$, equation (10a) becomes

$$\frac{D_j}{D_{30}} = 0.30(D_jV_j)^{1/2} + 0.0125\ D_jV_j \tag{11}$$

4759

A comparison of equation (11) with results obtained in reference 3 is given in the following table:

| Type of atomization | Exponents | |
|---|---|---|
| | $D_j$ | $V_j$ |
| 90° Impinging jets (eq. (11), for low injection velocities) | 0.5 | -0.5 |
| 180° Opposing jets (ref. 3) | 0.75 | -0.5 |

The velocity difference $\Delta V$ was found to have a pronounced effect on the atomization of impinging jets in airstreams for the range of conditions used in this investigation. A similar effect of the velocity difference between hot gases in a rocket engine and impinging jets therefore may be expected. The density of hot gases in a rocket engine is ordinarily about two times that of the airstream used in this investigation. Since $D_{30}$ was found to vary inversely with the 1/4 power of airstream density in reference 4, atomization of impinging jets in rocket engines may be expected to produce values of $D_{30}$ approximately 90 percent as large as those given in table I with other injection conditions similar. However, temperature conditions are considerably different in the present study. The high-temperature burning gases produced in a rocket engine can be expected to affect the distance or combustor length required for complete formation and vaporization. Thus, information is needed to establish relations between drop-size distributions for cold-flow and rocket-combustor conditions. Furthermore, studies of sprays in rocket engines are needed to determine quantitatively the effect of the high-temperature combustion environment on atomization and vaporization.


## SUMMARY OF RESULTS

Drop-size distributions produced by pairs of impinging n-heptane jets in airstreams were analyzed by using the following Nukiyama-Tanasawa drop-size-distribution expression:

$$\frac{dR}{dD} = \left(\frac{3.915}{D_{30}}\right)^6 \frac{D^5}{120} e^{-3.915\,D/D_{30}}$$

The effects of orifice diameter $D_j$, liquid-jet velocity $V_j$, and the velocity difference between the airstream and the liquid jets $\Delta V$ on the volume-number-mean drop diameter $D_{30}$ are given by the following empirical expression:

$$\frac{D_j}{D_{30}} = 2.64 \ \sqrt{D_j V_j} + 0.97 \ D_j \Delta V$$

where $D_j$ and $D_{30}$ are expressed in inches, and $V_j$ and $\Delta V$ in feet per second.

Lewis Flight Propulsion Laboratory
  National Advisory Committee for Aeronautics
    Cleveland, Ohio, December 19, 1957

## REFERENCES

1. Priem, Richard J.: Propellant Vaporization as a Criterion for Rocket-Engine Design; Calculations Using Various Log-Probability Distributions of Heptane Drops. NACA TN 4098, 1957.

2. Heidmann, Marcus F., Priem, Richard J., and Humphrey, Jack C.: A Study of Sprays Formed by Two Impinging Jets. NACA TN 3835, 1957. (Supersedes NACA TN 2349.)

3. Tanasawa, Yasusi: The Atomization of Liquid by Means of Flat Impingement. Preprint No. 356-56, Am. Rocket Soc., 1956.

4. Ingebo, Robert D., and Foster, Hampton H.: Drop-Size Distribution for Crosscurrent Breakup of Liquid Jets in Airstreams. NACA TN 4087, 1957.

5. Ingebo, Robert D.: Vaporization Rates and Drag Coefficients for Isooctane Sprays in Turbulent Air Streams. NACA TN 3265, 1954.

6. Bevans, Rowland S.: Mathematical Expressions for Drop Size Distribution in Sprays. Conf. on Fuel Sprays, Univ. of Michigan, Mar. 30-31, 1949.

4759

4417

CB-2

TABLE I. - TEST CONDITIONS FOR MAXIMUM-OBSERVED

AND MEAN DROP DIAMETERS

[Airstream temperature, 82° F; airstream
static pressure, 29.3 in. Hg abs.]

| Run | Liquid-jet velocity, ft/sec | Airstream velocity, ft/sec | Injector orifice diameter, in. | Maximum-observed drop diameter, microns | Volume-number-mean drop diameter, microns |
|---|---|---|---|---|---|
| 1 | 65 | 65 | 0.089 | 1160 | 347 |
| 2 | ↓ | ↓ | .060 | 850 | 293 |
| 3 | ↓ | ↓ | .029 | 700 | 200 |
| 4 | 100 | 100 | .029 | 560 | 162 |
| 5 | 100 | 65 | 0.029 | 435 | 134 |
| 6 | 65 | 100 | ↓ | 500 | 160 |
| 7 | ↓ | 180 | ↓ | 300 | 113 |
| 8 | ↓ | 300 | ↓ | 180 | 68 |
| 9 | ↓ | 100 | .060 | 575 | 212 |
| 10 | ↓ | 180 | ↓ | 325 | 131 |
| 11 | ↓ | 300 | ↓ | 190 | 79 |
| 12 | ↓ | 100 | .089 | 750 | 240 |
| 13 | ↓ | 180 | ↓ | 375 | 142 |
| 14 | ↓ | 300 | ↓ | 250 | 87 |
| 15 | 30 | 65 | .029 | 760 | 270 |
| 16 | 30 | 180 | .029 | 340 | 126 |
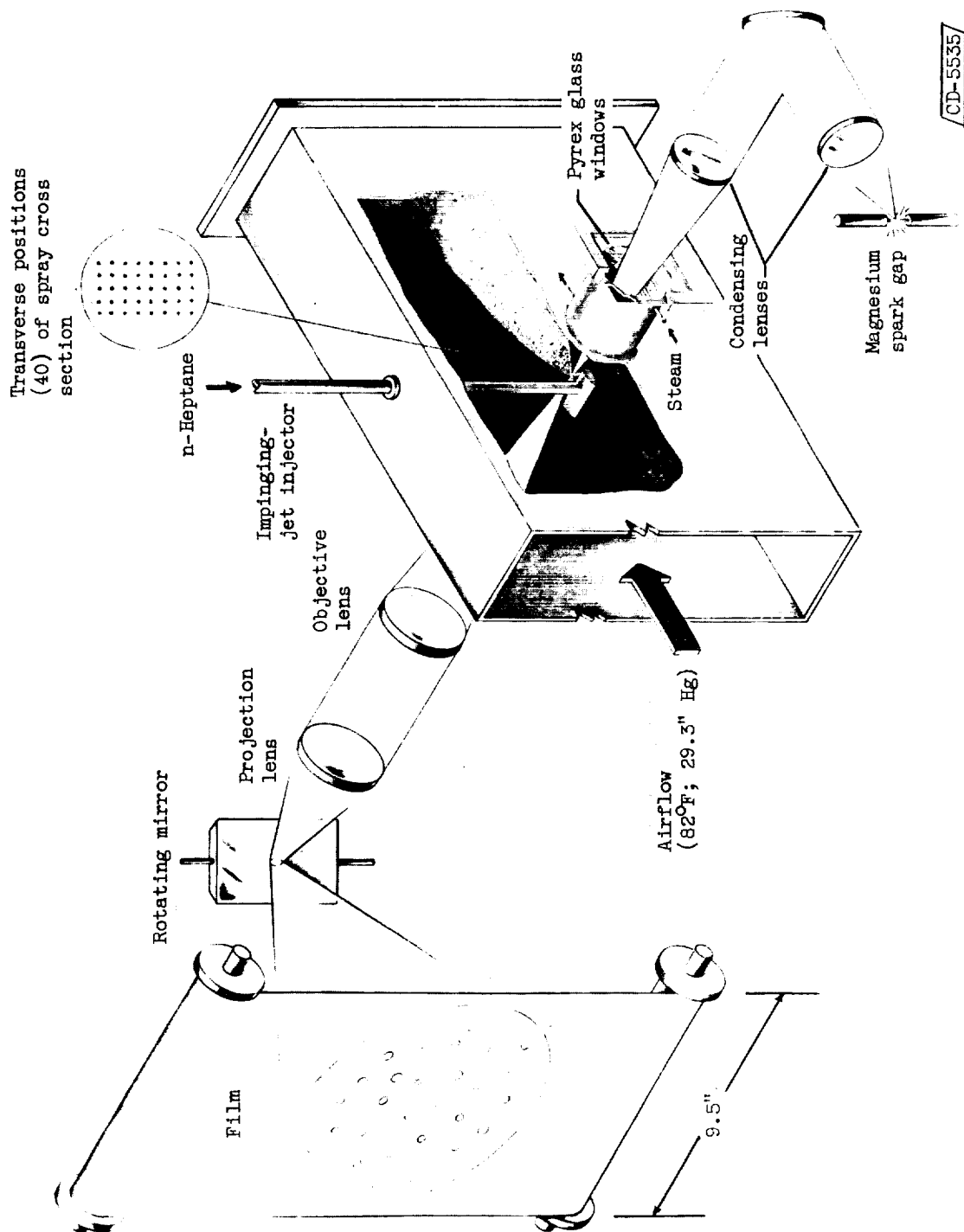
Figure 1. Test section and equipment.

0.9 in.

0.25 in.

45°

45°

2.5 in.

1/8 in. Inconel tube;
0.018 in. wall
0.089 in. I. D

0.50 in.

1.45 in.

1/2 in. Inconel tube;
1/16 in. wall

Airflow
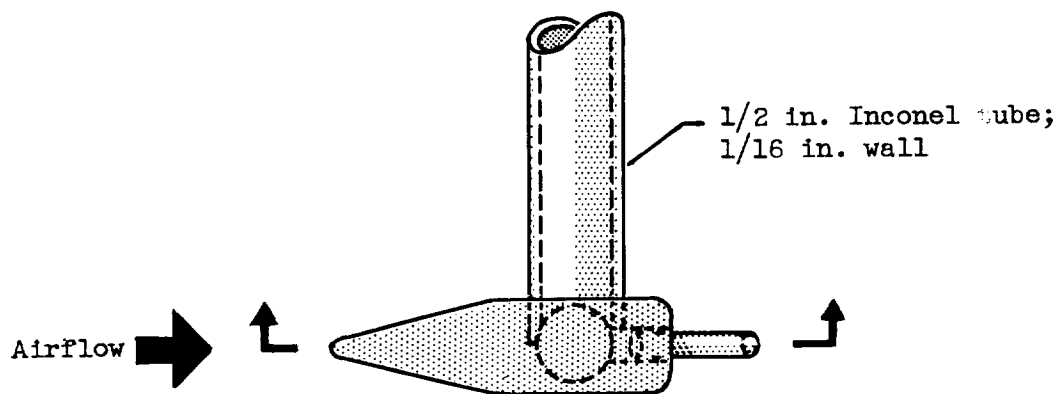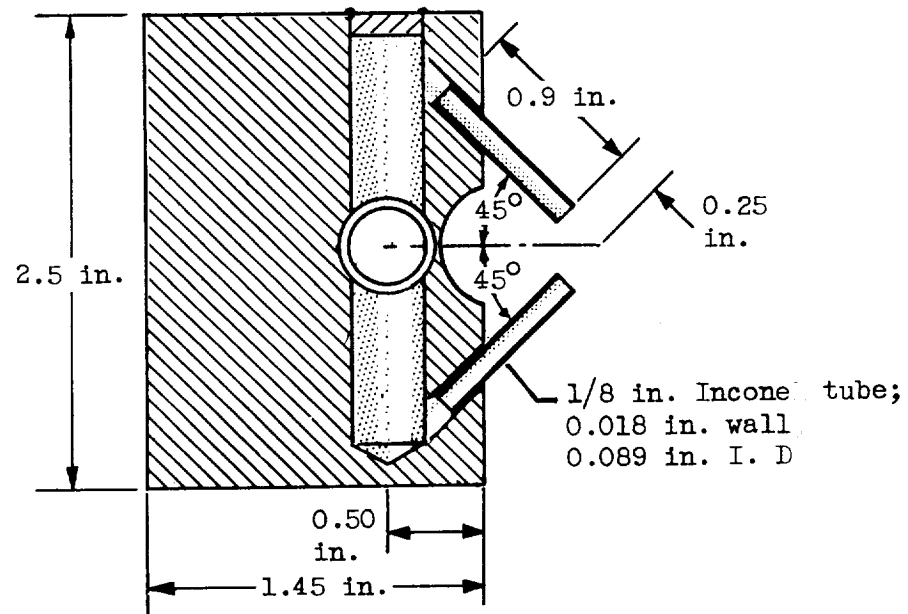
CD-5902

(a) Large injector.

Figure 2. - Impinging-jet injectors.

Airflow

1/2 in. Inconel tube;
1/32 in. wall

1/8 in. Inconel tubes;
1/32 in. wall

1/4 in. steel rod

1/4 × 3/8 × 4 in. steel bar

0.25 in.

59° taper

0.55 in.

45°    45°

1/4 in.

1¼ in. rad.

1/4 in.

CD-5903

0.029- or .060 in. diameter

Brass orifice tips;
two interchangeable pairs
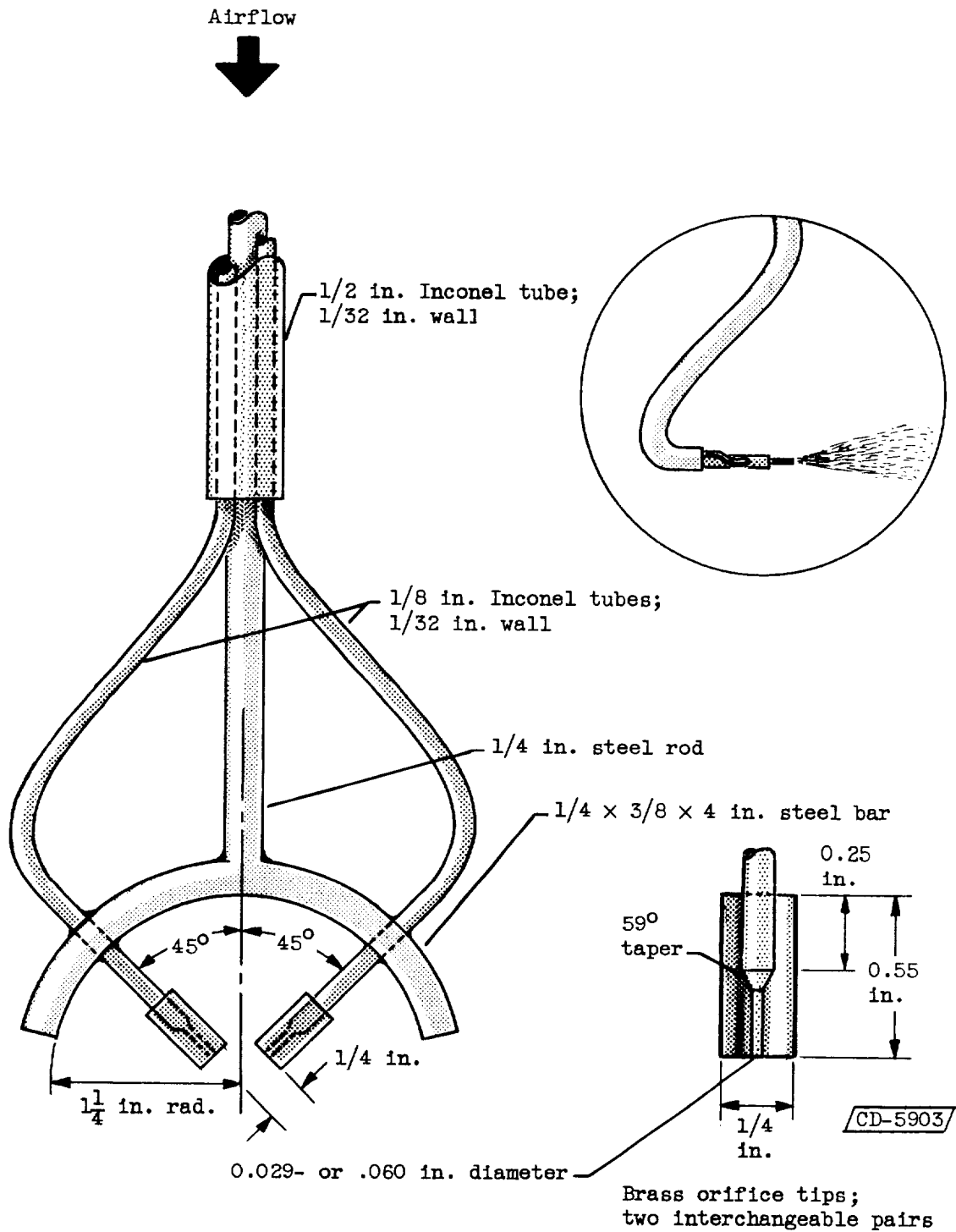
(b) Medium and small injectors.

Figure 2. - Concluded.  Impinging-jet injectors.

4759
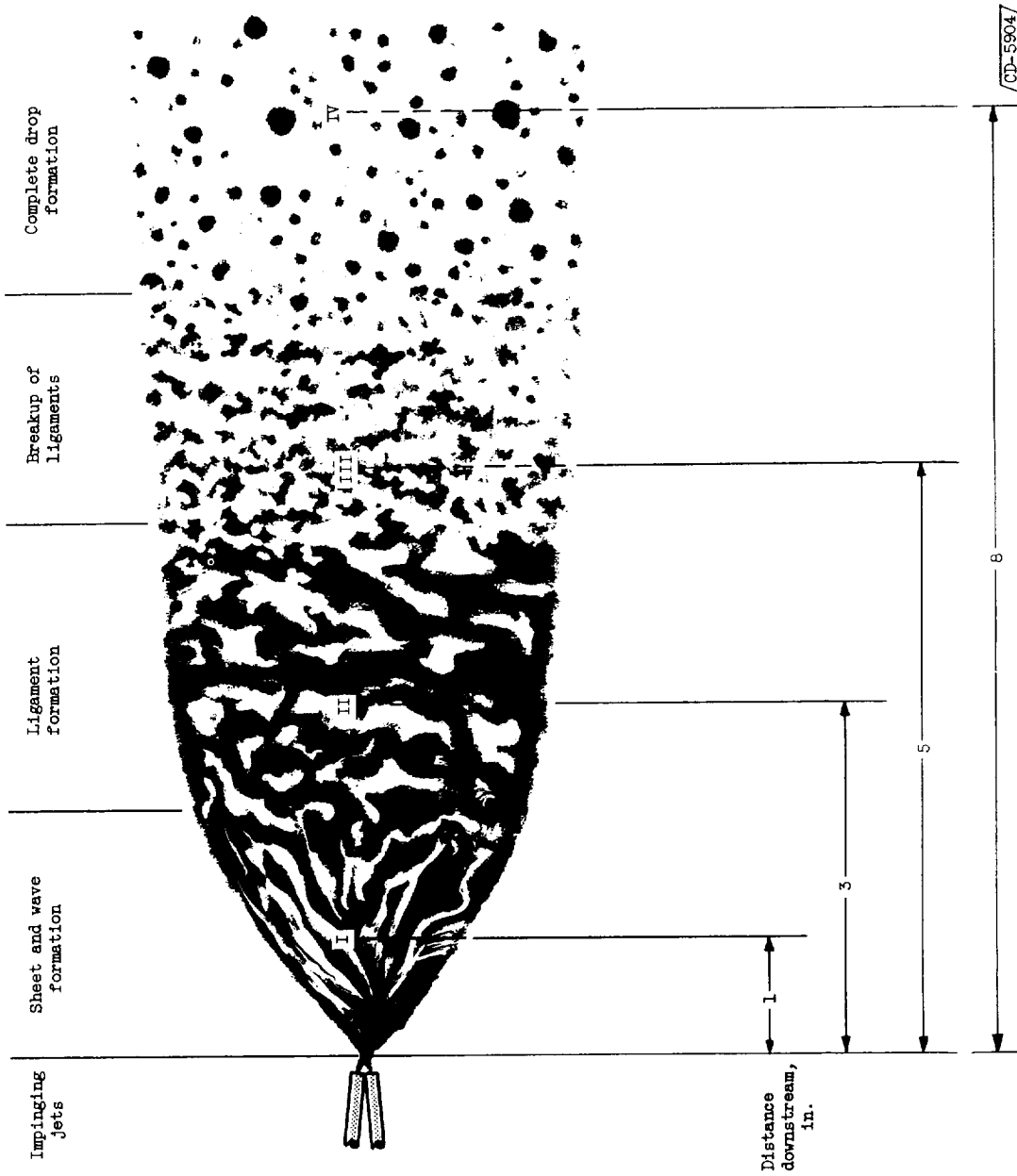


(a) Schematic representation of atomization using impinging jets.

Figure 3. - Atomization process for impinging jets.

(b) Sheet and wave formation, 1 inch from point of impingement (zone I); ×21.
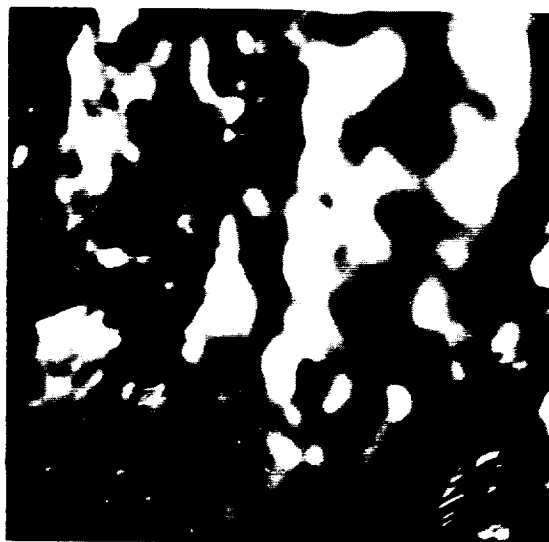


(c) Ligament formation, 3 inches from point of impingement (zone II); ×21.
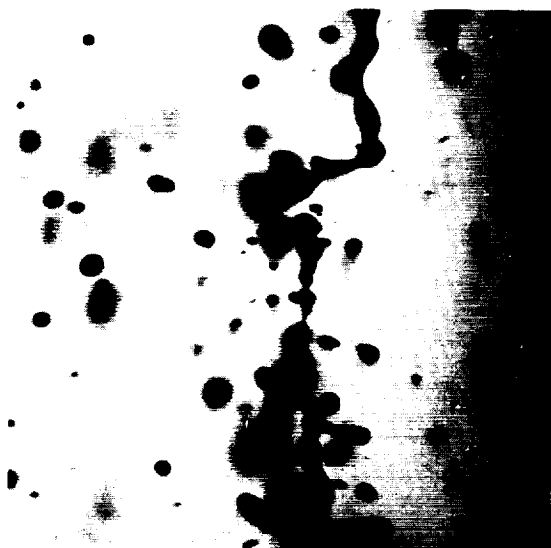


(d) Breakup of ligaments, 5 inches from point of impingement (zone III); ×21.



(e) Complete drop formation, 8 inches from point of impingement (zone IV); ×21.

Figure 3. - Concluded.  Atomization process for impinging jets.

4759
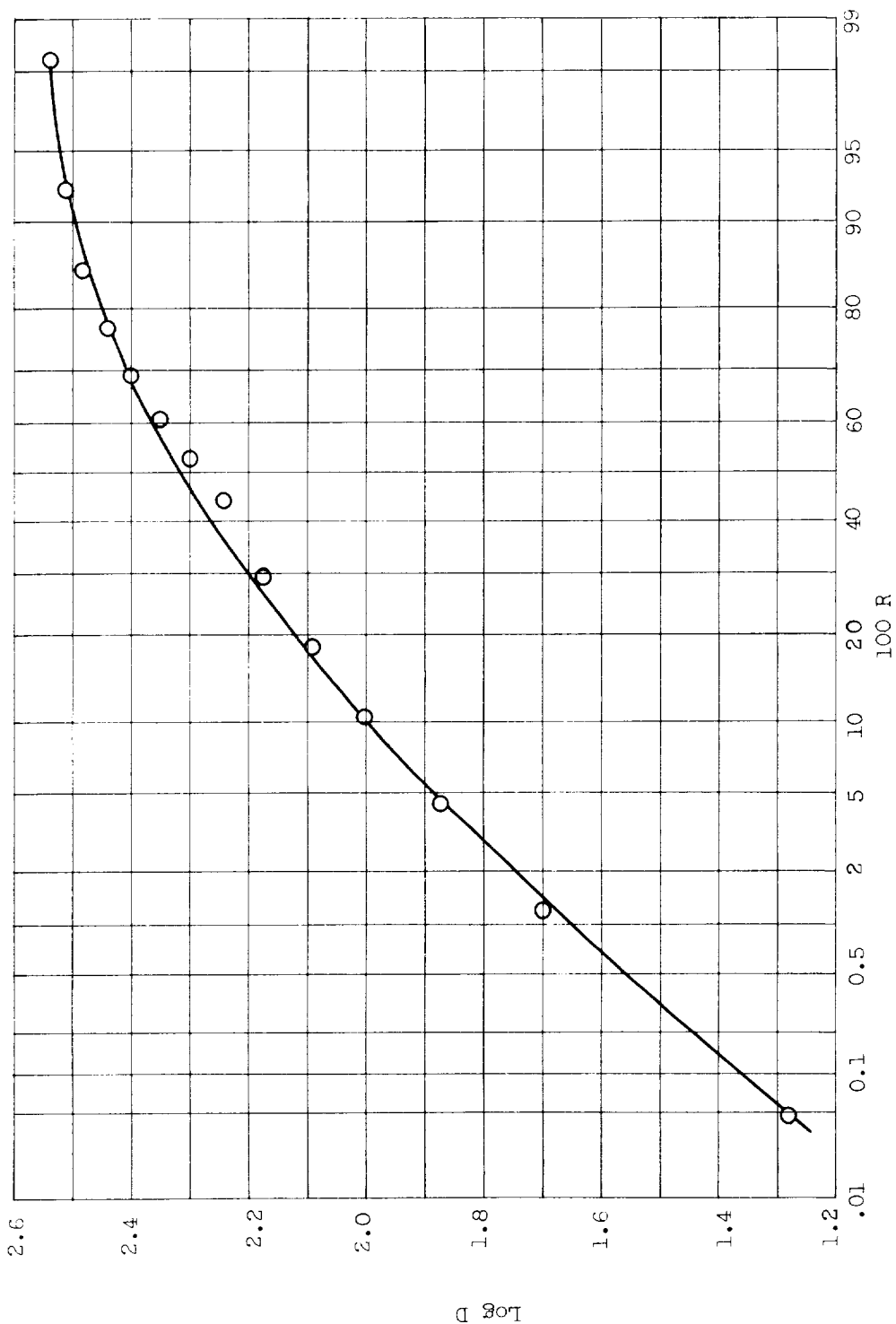


(a) Log-probability analysis. Orifice diameter, 0.089 inch.

Figure 4. - Atomization of impinging liquid jets. Liquid jet velocity, 65 feet per second; airstream velocity, 180 feet per second.
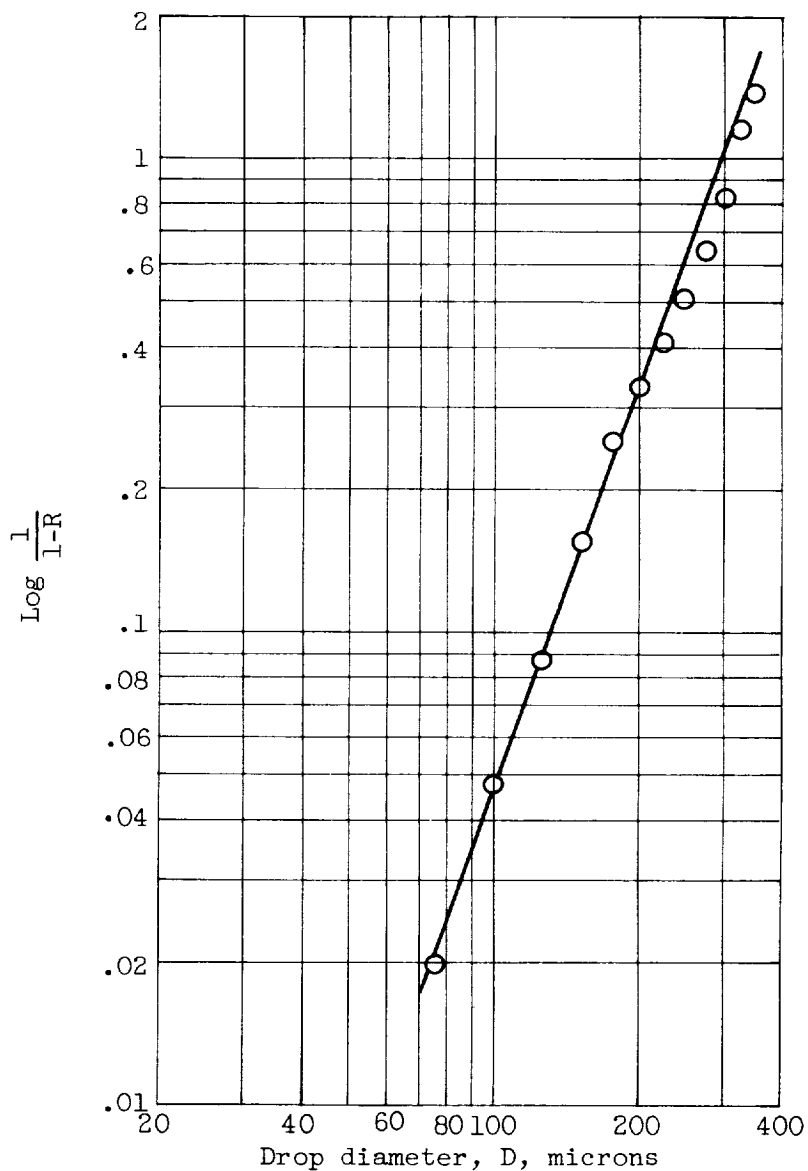
(b) Rosin-Rammler analysis.  Orifice diame-
ter, 0.089 inch.

Figure 4. - Continued.  Atomization of im-
pinging liquid jets.  Liquid jet velocity,
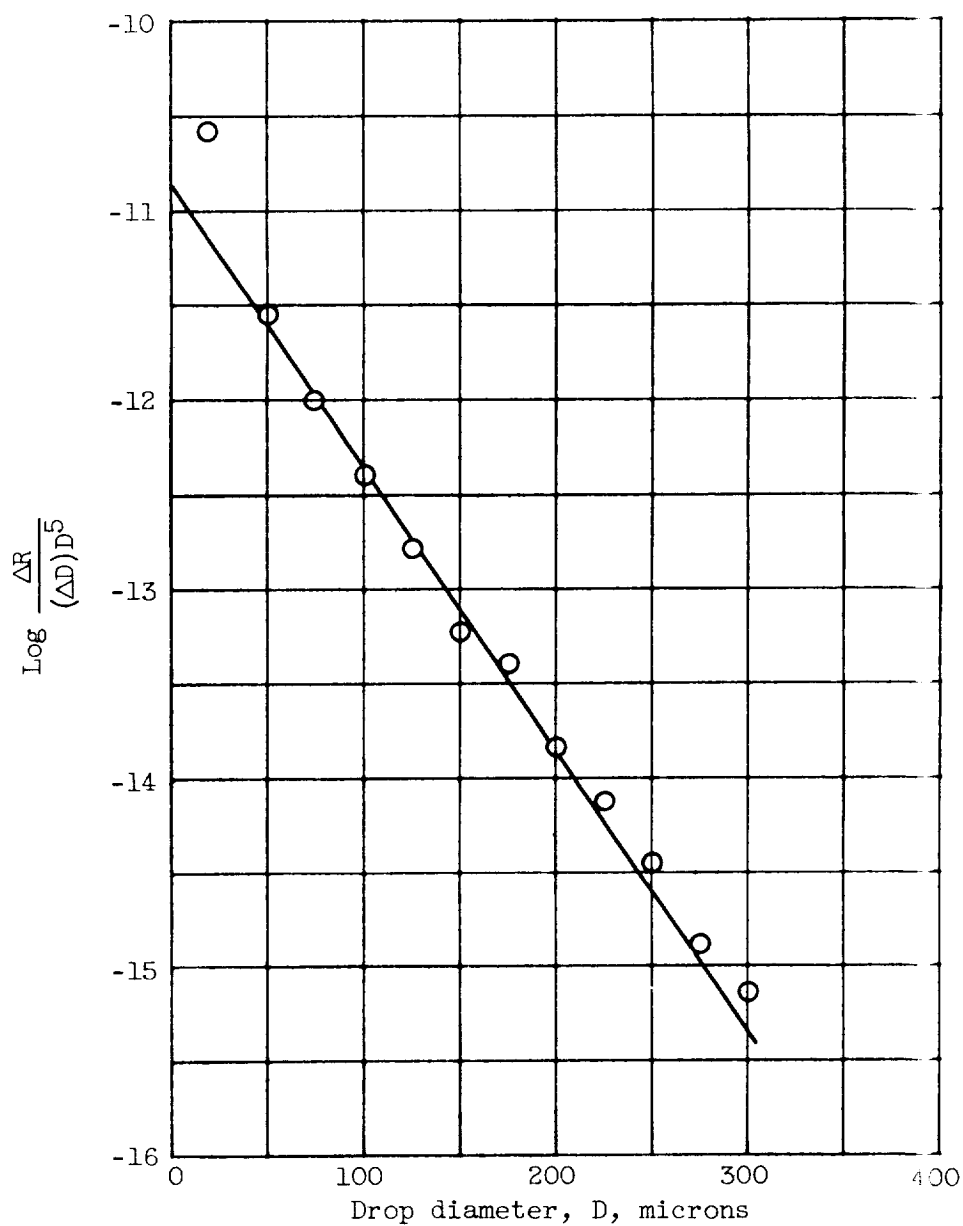65 feet per second; airstream velocity,
180 feet per second.

4759

CB-3
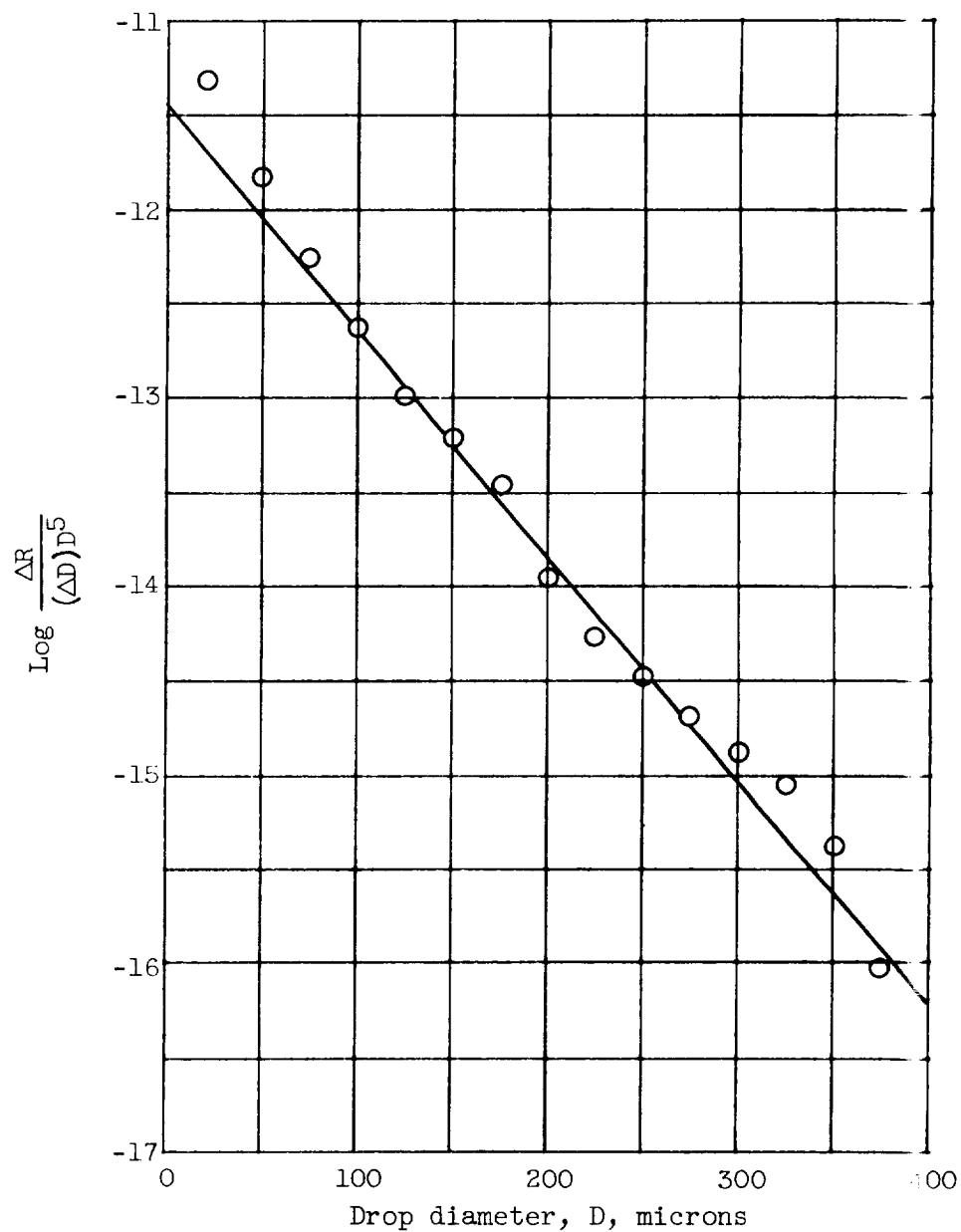


(c) Nukiyama-Tanasawa analysis.  Orifice diameter,
   0.089 inch; $D_{30}$, 142 microns.

Figure 4. - Continued.  Atomization of impinging
   liquid jets.  Liquid jet velocity, 65 feet per
   second; airstream velocity, 180 feet per second.
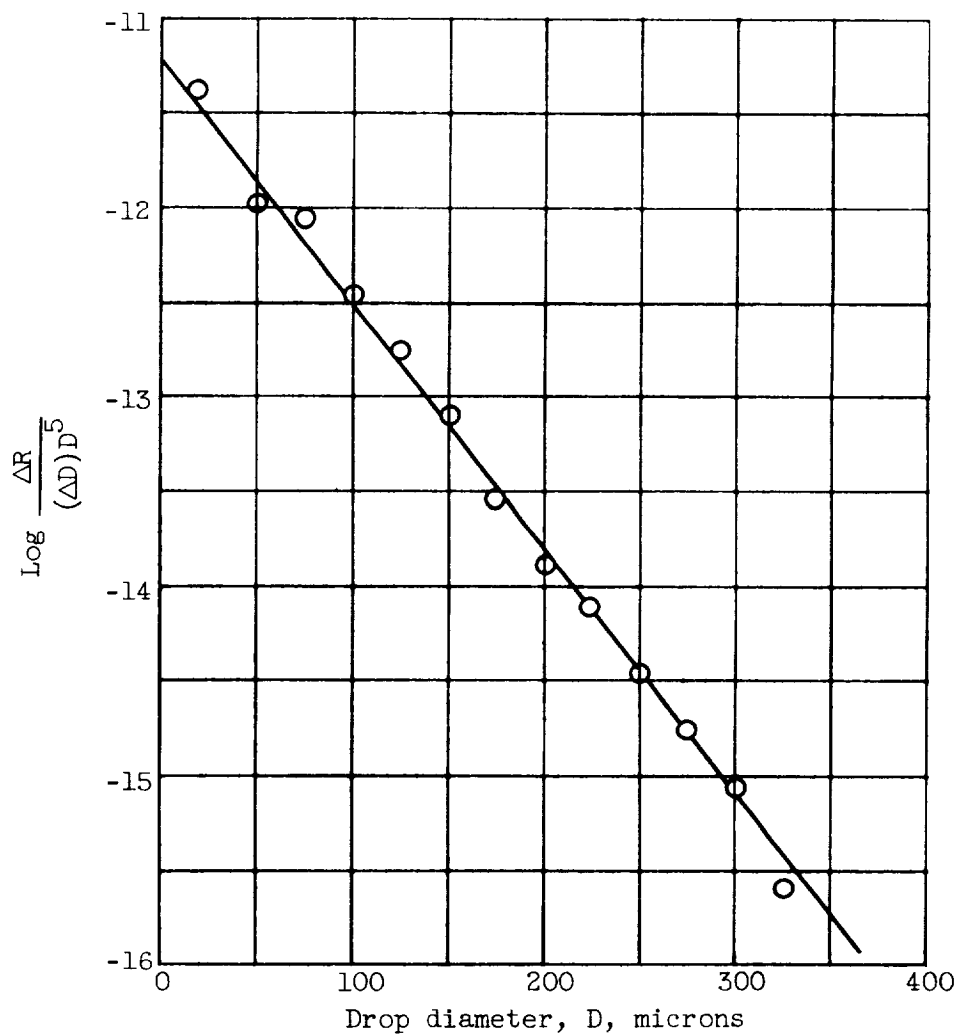
(d) Nukiyama-Tanasawa analysis.  Orifice diameter,
    0.060 inch; $D_{30}$, 131 microns.

Figure 4. - Continued.  Atomization of impinging
    liquid jets.  Liquid jet velocity, 65 feet per
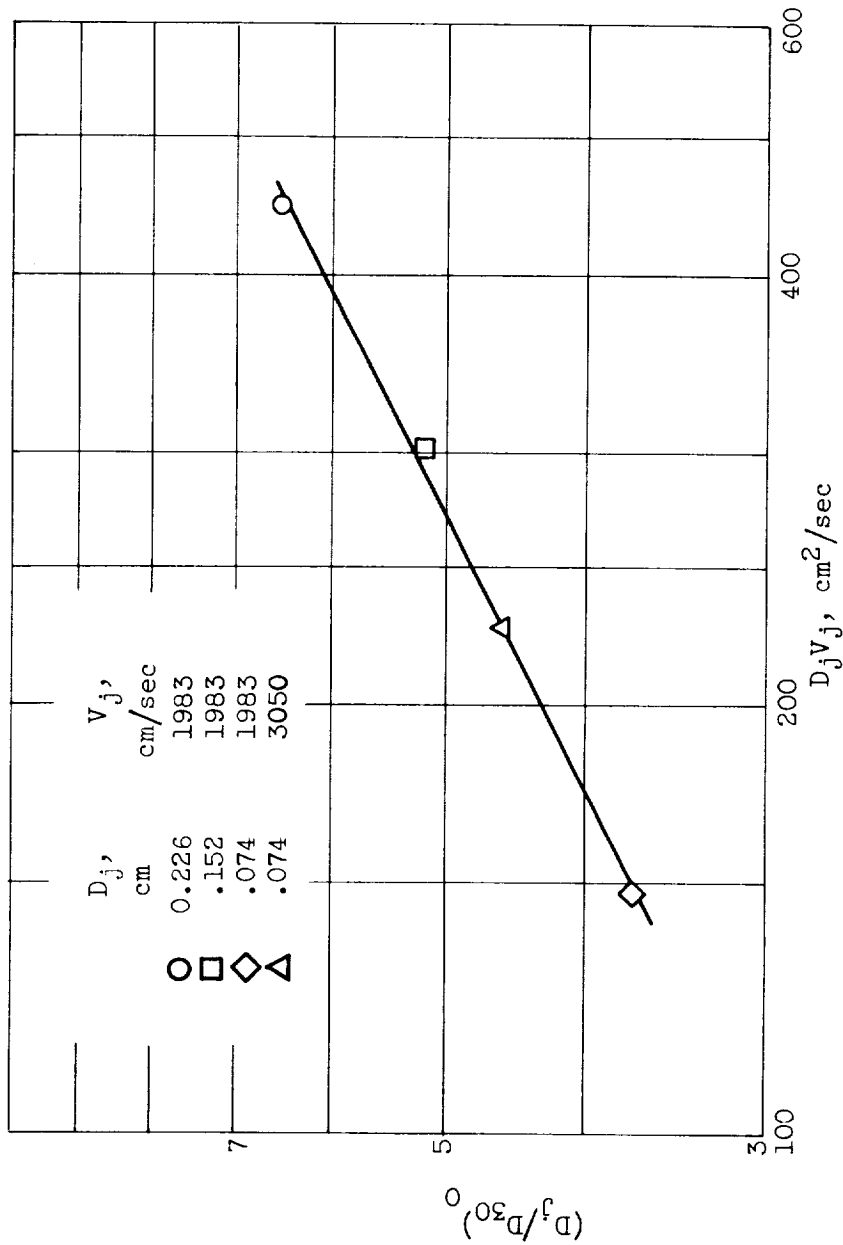    second; airstream velocity, 180 feet per second.

(e) Nukiyama-Tanasawa analysis.  Orifice diameter, 0.029 inch; $D_{30}$, 113 microns.

Figure 4. - Concluded.  Atomization of impinging liquid jets.  Liquid jet velocity, 65 feet per second; airstream velocity, 180 feet per second.

Figure 5. - Relation between volume-number-mean drop diameter $D_{30}$, orifice diameter $D_j$, and liquid-jet velocity $V_j$ when airstream velocity and liquid-jet velocity are equal ($\Delta V = 0$).
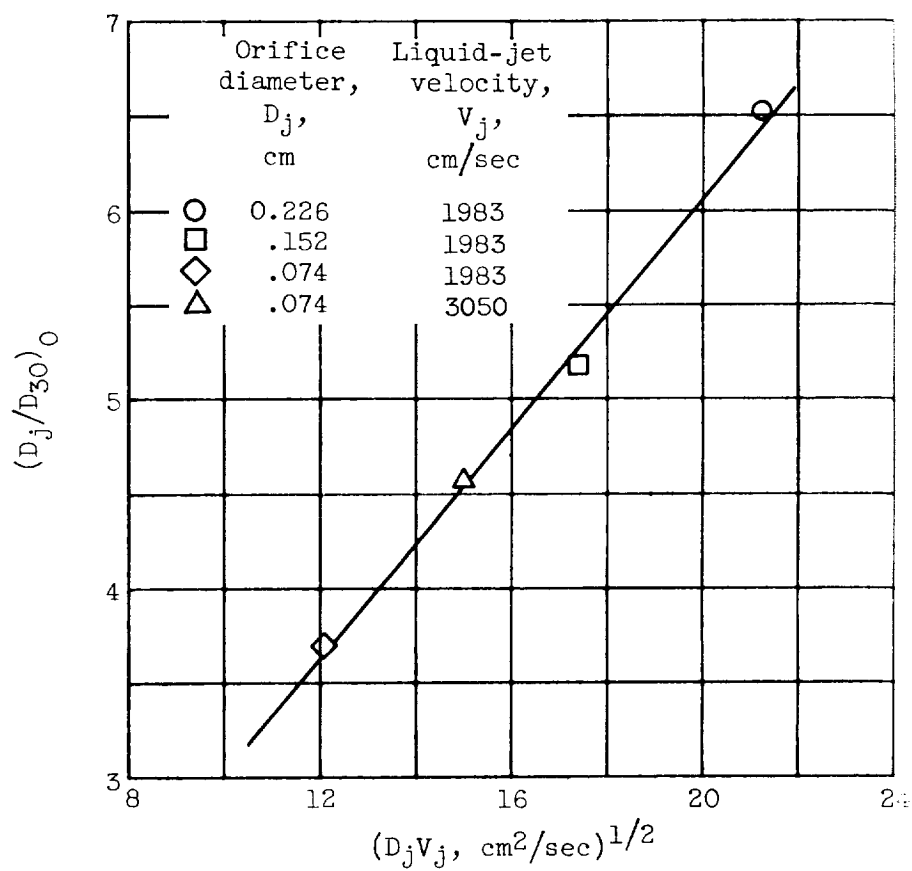
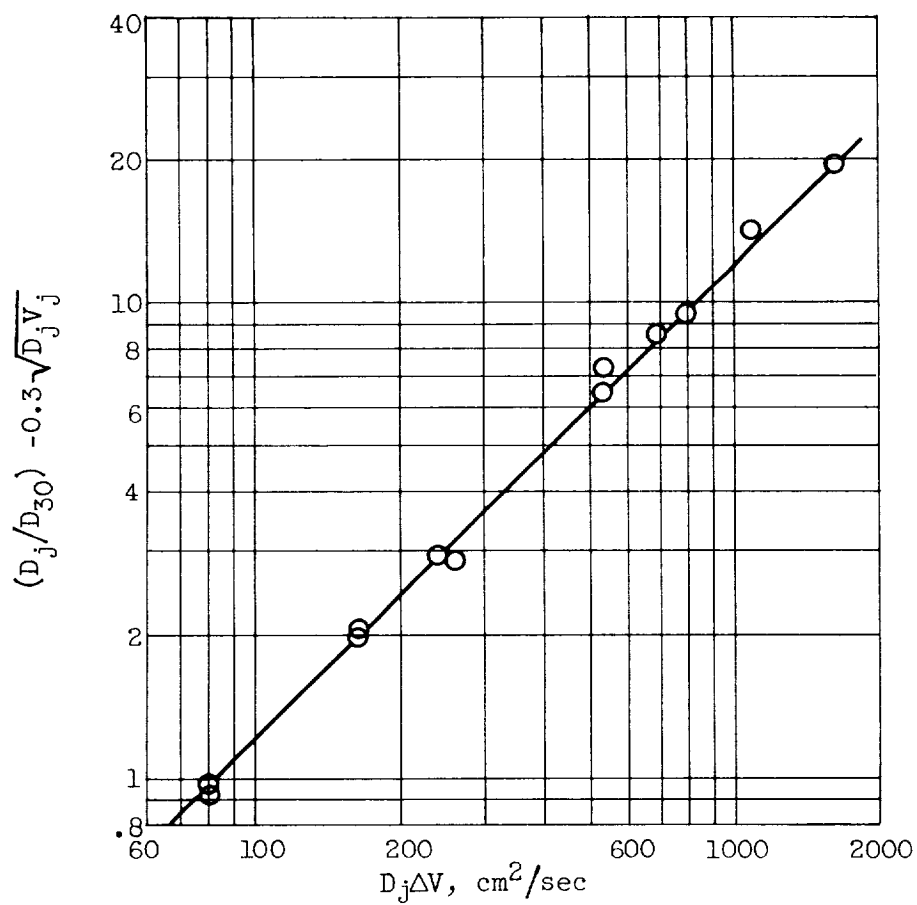Figure 6. - Evaluation of proportionality constant $K_1$.

Figure 7. - Relation between volume-number-mean
drop diameter $D_{30}$, orifice diameter $D_j$, liquid-
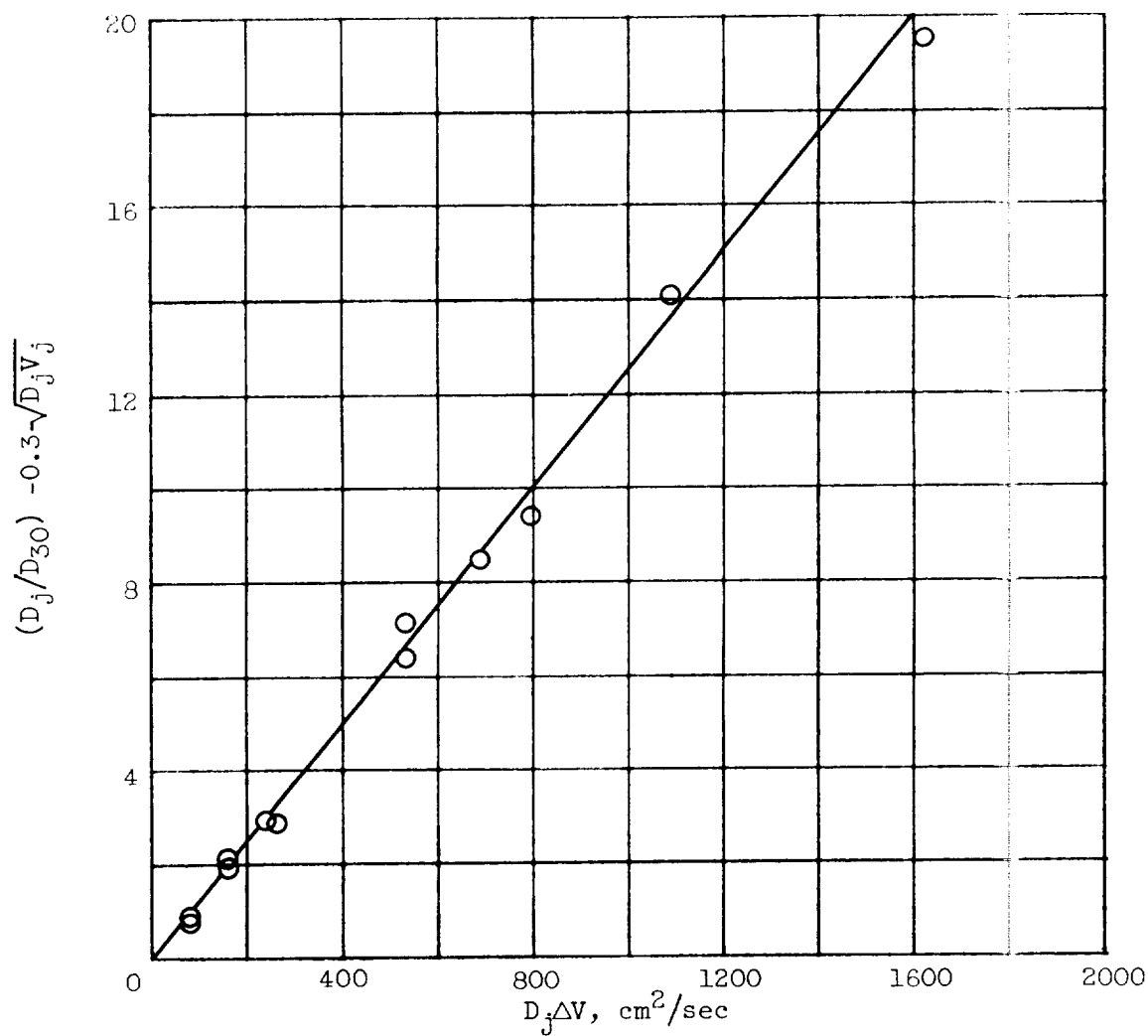jet velocity $V_j$, and velocity difference $\Delta V$.

4759



Figure 8. - Evaluation of proportionality constant $K_2$.